journal of the mechanical behavior of biomedical materials 134 (2022) 105369

Contents lists available at ScienceDirect

Journal of the Mechanical Behavior of Biomedical Materials

journal homepage: www.elsevier.com/locate/jmbbm

Modeling, design and tailoring of a tough, strong and stiff multilayered bone graft material

Seyed Alireza Mirmohammadi [a], Damiano Pasini [a], Francois Barthelat [a,b,*]

[a] Department of Mechanical Engineering, McGill University, Montreal, Quebec, Canada
[b] Department of Mechanical Engineering, University of Colorado, Boulder, CO, USA

A B S T R A C T

Damage tolerance, stiffness, and strength are critical mechanical properties that are difficult to achieve concurrently in synthetic monolithic materials. This limits the range of certain applications, including in bone graft materials where bone-like mechanical reliance is desired. For example, calcium sulfate (CS) is a biologically compatible ceramic that possesses several properties of an ideal bone graft material, but its applications in medicine is limited by its brittleness. Brittleness may be alleviated by the addition of stronger and more ductile reinforcements, with the best mechanical improvements obtained when the layered architecture and the interfaces for these reinforcements are tailored. Here we propose a systematic modeling and design approach to tailor the architecture and properties of a multilayered bone graft material composed of a brittle ceramic and a more ductile material such as metals. More specifically, the volume fraction, moduli, number of layers, and the toughness of the interfaces between the different phases are tailored to maximize overall stiffness, strength, and energy absorption capacity. Our model predicts that when the stiffness of the reinforcement is higher (lower) than the ceramic, the beams with lower (higher) number of layers and higher (lower) volume fraction of metal are stronger. However, while the higher number of layers is always desired in terms of energy dissipation, the effects of other variables is more complex to understand and should thus be studied in conjunction with each other.

1. Introduction

Simple homogenous materials cannot meet the ever-increasing demand for materials with high performance as some of their mechanical properties, such as resistance to permanent deformation (strength), resistance to recoverable deformation (stiffness), and resistance to fracture (toughness) are mutually exclusive (Ritchie, 2011). For example, while ceramics are both strong and stiff, their vulnerability to crack growth limits their application as bone graft materials, where high energy absorption is a requirement. Calcium sulfate (CS) is a brittle bioceramic that offers many properties of an ideal bone graft material, namely bioresorbability, biocompatibility, and osteoconductivity (Moussa et al., 2020). Yet, its mechanical properties do not approach those of natural bone (Anusavice et al., 2012). Low fracture resistance, strength and stiffness are the drawbacks of CS that limit its use in several applications. There are two powerful strategies to toughen ceramics. First, toughness can be improved by incorporating metallic reinforcements. The metallic phase can be in the form of particles (Krstic, 1983), fibers, whiskers (Zok and Hom, 1990), and layers (Chen and Mecholsky, 1993), oriented ideally across the expected trajectory of cracks. While the (brittle) ceramic component may partially crack, the traction applied on the crack faces by the metallic phase can remain intact, thus bridging the crack and hindering its advancement (Zok and Hom, 1990; Hwu and Derby, 1999). Crack bridging has successfully been used to overcome the brittleness of ceramic materials (Chen and Mecholsky, 1993; Humburg et al., 2014; Cavelier et al., 2021; Li and Soboyejo, 2000). A second strategy is to form ceramics into multilayered architectures, where weaker interfaces between layers can deflect cracks from their main path. This strategy is exploited in biological materials, such as bone (Koester et al., 2008), and mineralized natural materials, such as nacre (Khayer Dastjerdi et al., 2013), to attain unusual combination of strength and toughness. The interfaces keeping the building blocks together hamper crack propagation, control the deformation and failure mechanisms in different levels of the hierarchy, and enable the natural materials to dissipate a large amount of energy (Barthelat, 2015; Barthelat et al., 2016). Moreover, not only do the interfaces at different hierarchical levels of the bone play a key role in deflecting the propagating cracks (Koester et al., 2008), but also the non-collagenous proteins accumulated in these interfaces contribute to the overall toughness of the bone (Thurner et al., 2010). In layered ceramics, the incoming crack deviates into the interface, unlike monolithic ceramic materials in which the crack propagates in a catastrophic and unstable manner, where its growth is more stable (Ritchie, 2011). Experimental results suggest that crack deflection is a powerful strategy to increase the

* Corresponding author. Department of Mechanical Engineering, McGill University, Montreal, Quebec, Canada.
E-mail address: francois.barthelat@colorado.edu (F. Barthelat).

https://doi.org/10.1016/j.jmbbm.2022.105369
Received 30 May 2022; Accepted 9 July 2022
Available online 16 July 2022
1751-6161/

toughness of ceramic materials and avoid catastrophic failure (Humburg et al., 2014; Lenčéš et al., 2000; Ye et al., 2015; Wang et al., 2002; Clegg et al., 1990; Zhang et al., 2014; Tomaszewski et al., 2007; Kovar et al., 1998).

One approach to optimize the performance of layered materials is to have control over the structure, geometry, arrangement and size of the constituent phases, thereby activating toughening mechanisms. For instance, it has been demonstrated that the mechanical properties of nitride/boron nitride (Zan et al., 2004), and alumina/aluminum, alumina/copper and alumina/nickel layered structures (Hwu and Derby, 1999) depend on design parameters. In this regards, several models have also been developed to study the fracture behavior of laminated ceramics. He and Hutchison (Ming-Yuan and Hutchinson, 1989) determined the condition for crack deflection: the fracture toughness of the brittle interface should be less than 25% of that of the elastic layers. Kovar et al. (1998) suggested that a high energy absorption capacity can be potentially achieved in layered ceramics with optimum interfacial fracture resistance. Philisps et al. (Phillipps et al., 1993) and Folsom et al. (1994a) modeled the flexural behavior of different laminate ceramics. These models were supported by experimental results obtained for *SiC*/graphitic (Clegg et al., 1990) glass/thermoplastic and alumina/carbon-reinforced composite (Folsom et al., 1994b). A similar model was also proposed to study the bending behavior of alumina/lanthanum phosphate laminate composite (Dey et al., 2008). The discrete element method (Zhang et al., 2014) has also been used to study the fracture behavior of *SiC–C* laminate with graphite as the weak interface.

Understanding the failure behavior of a multilayered composite and replicating the fracture features of such structures including crack propagation, crack deflection, delamination with the purpose of combining conflicting mechanical properties is still elusive in the literature. In this paper, we develop a numerical model to study the fracture behavior and tune the design variables of a multilayered composite comprising alternating ceramic and metallic layers. The model enables us to investigate the effect of crack deflection and crack bridging on the failure response of the multilayered composite. The model can be used to explore the design space of a multilayered bone graft material where a combination of strength, stiffness, and energy dissipation can be achieved concurrently. More specifically, the model generates guidelines to promote both crack deflection and crack bridging in a multilayered metal/ceramic bone graft material so that its mechanical properties approach those of an ideal bone substitute.

2. Description of the numerical model

A critical element in the design and tailoring of the architecture of multilayered bone graft material is a robust and accurate model that can predict the deformation and fracture of a ceramic/metal multilayered beam. In this study we focus on bending, which is representative of a typical loading that long bone grafts experience. The main objective of the model is to identify the multilayered architecture that leads to the highest combinations of stiffness, strength and toughness, in a three-point bending loading configuration. Our reference material is a pure homogeneous ceramic and we aim at improving its flexural properties by introducing metallic layers. The material properties and design parameters for the multilayered beam are: (i) the modulus of the ceramic E_c and the metallic layers E_m, (ii) the volume fraction of the metallic phase φ, (iii) the number of ceramic layers N_c (= N_m-1), (v) and the toughness of the interface. The width and length of the beam are prescribed as b and $2L$ respectively. Fig. 1a shows the geometrical parameters.

We first develop a model that captures the elastic response, and then the progressive crack propagation in a multilayered bone graft beam subjected to three-point bending. We make the following assumptions:

1 Planar domain under plane-stress condition. Small deformation for both the metal and ceramic material, hence assumed as linear elastic. The maximum tensile stress criterion governs the brittle fracture of

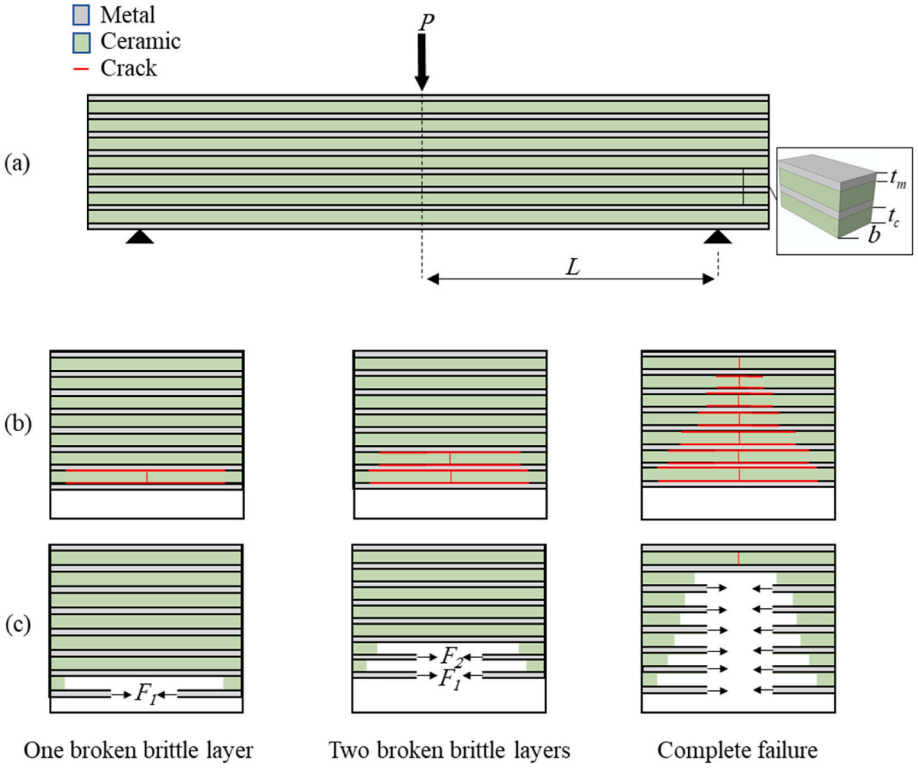

Fig. 1. (a) the multilayered beam is subjected to three-point bending loads. (b) four cracks symmetrically propagate along the interfaces immediately after the failure of each ceramic layers (c) the debonded metallic ligaments are replaced with their equivalent forces.

the ceramic. When the maximum tensile stress in a given ceramic layer reaches its tensile strength S_c ($S_c/E_c = 0.001$), the layer fails due to brittle fracture in the center of the beam. The fracture of the last ceramic layer leads to the complete failure of the beam.

2 Two events are triggered by the fracture of the individual ceramic layers: (i) the ceramic layer immediately fractures across its thickness but the crack is arrested by the next metallic layer and (ii) because of the stress singularity at the tip of the crack, symmetric delamination cracks immediately occur in the transverse direction (Fig. 1).

3 As a crack propagates across the layers, the neutral axis of the beam shifts, but the strain distribution across the sections of the intact layers of the beam remains a linear function of the distance from the neutral axis.

4 An energy criterion governs interfacial crack propagation. Cracks symmetrically propagate along the interface towards the ends of the beam until the energy release rate is equal to its critical value G_c. The toughness of the interface is assumed to be constant along the interface as the cracks extend (Phillipps et al., 1993). We also assume that at each stage of crack propagation, the newly formed interfacial cracks are the first cracks that propagate followed by the propagation of previously formed cracks.

5 Ceramic layer portions between two adjacent interfacial cracks no longer carry load. This assumption accounts for the effect of interfacial crack growth on the compliance of the beam. Their contribution to the bending compliance is neglected (Phillipps et al., 1993).

6 Debonded sections of the metallic layers carry only tensile stresses. Frictional effects between the debonded metallic layers and the ceramic layers are neglected.

3. Elastic response

To obtain the force-deflection diagram of a multilayered beam under three-point bending loading, we first consider an intact beam (Fig. 1a). Through Euler–Bernoulli beam theory beam theory, the force P as a function of the applied deflection δ is given by:

$$P = \frac{6\delta(EI)_{eq}}{L^3} \tag{1}$$

where $(EI)_{eq}$ is the effective flexural stiffness of the whole beam. The neutral axis is located exactly half way across the intact beam due to symmetry of the geometry, loading and boundary conditions. Using the parallel axis theorem, the expression for the effective flexural stiffness can be written as:

$$(EI)_{eq} = E_m \sum_{j=1}^{N_m} \left(\overline{I_m} + A_m h_j^2\right) + E_c \sum_{j=1}^{N_c} \left(\overline{I_c} + A_c h_i^2\right) \tag{2}$$

where h_j and h_i are respectively the distances of the midline of jth metallic layer and ith ceramic layer to the neutral axis. $\bar{I}$ and A are respectively the moment of inertia of each layer about its central line and area of the layer. Our reference response is a beam with identical size made entirely of ceramic. The normalized effective flexural stiffness can then be written as:

$$\frac{(EI)_{eq}}{(EI)_c} = \frac{12}{bt^3}\left(\frac{E_m}{E_c}\sum_{j=1}^{N_m}\left(\overline{I_m} + A_m h_j^2\right) + \sum_{j=1}^{N_c}\left(\overline{I_c} + A_c h_i^2\right)\right) \tag{3}$$

Fig. 2 shows a plot of the normalized effective flexural stiffness, Eq. (3), as a function of the elastic modulus ratio for given number of layers and volume fractions of the metallic phase. In this figure, φ is the volume fraction of the metallic phase. For $E_m/E_c = 10$, the lower the number of layers, the higher the effective flexural stiffness of the beam would be, because thicker layers are placed far from the neutral axis. Additionally, the effective flexural stiffness of the beam is linearly proportional to the volume fraction of the stiff metal because as the volume fraction of the reinforcement increases, a higher portion of the beams is made of the stiffer. In contrast, incorporating a metal with low effective stiffness ratio into the ceramic ($E_m/E_c = 0.1$) has a reverse impact on the effective flexural stiffness of the beam.

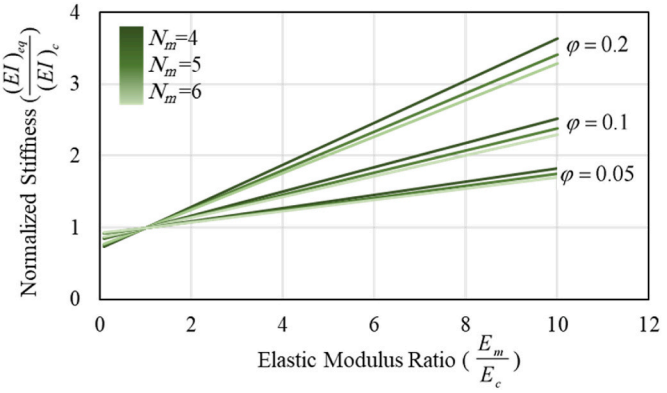

Fig. 2. Nondimensional effective flexural stiffness as a function of the volume fraction of the metal for different number of layers. φ represents the volume fraction of the reinforcement.

The role of the number of layers on the stiffness is in accordance with the experimental results presented in a previous work (Cavelier et al., 2021), where we experimentally investigated the effect of design parameters on the mechanical properties of titanium (Ti) mesh-reinforced CS multilayers.

Since to maximize the dissipated energy and strength, we need to consider the entire force-deflection curve of the multilayer used, we now turn our attention to the post fracture behavior of the beam. We begin our analysis by considering a multilayered beam with only one broken ceramic layer. Then, we consider further crack propagation and we extend the model to analyze a beam with N_{broken} cracked ceramic layers. These sequences are illustrated in Fig. 1b and c.

3.1. Failure of one ceramic layer

The elastic response of the beam ends when the flexural stress in the ceramic phase reaches the tensile strength of the ceramic. Because of the loading configuration, this occurs first at the lowermost ceramic layer (Fig. 1b). Once the first ceramic layer breaks, symmetric delamination cracks immediately propagate along the interface between the broken ceramic layer and the adjacent metallic layers.

The fracture of the first ceramic layer and the interfacial crack propagation lead to a redistribution of stresses in the beam. The debonded parts of the ceramic placed between the tips of the interfacial cracks and the through-thickness crack (damaged region) cease to carry any loads (white area in Fig. 3a). However, a metallic ligament is assumed to remain, carrying a tensile F_1 as shown in Fig. 3b. These failure events shift the position of the neutral axis, and the intact ligament in the multilayered beam is assumed to behave elastically. In addition, because the delamination crack propagates in a finite region, the zones near the ends of the beam remain intact; this enables to divide the beam into a damaged zone and an intact zone (Fig. 3a). The flexural stiffness of the beam in the damaged region can be written as:

$$(EI)_1 = E_m \sum_{j=2}^{N_m} \left(\overline{I_m} + A_m h_j^2\right) + E_c \sum_{j=2}^{N_c} \left(\overline{I_c} + A_c h_i^2\right) \tag{4}$$

where h_i and h_j respectively indicate the distance of ith ceramic and jth metallic layers to the neutral axis. The location of the neutral axis in the damaged region can be found using the equation of equilibrium of forces acting on the cross section A-A. The force F_1 carried by the debonded metallic layer (Fig. 3) can be found from:

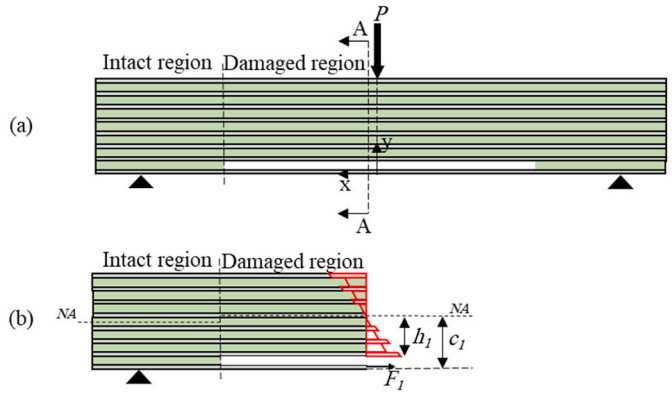

Fig. 3. (a) Schematic representation of the beam with one broken ceramic layer divided into 2 regions (b) stress distribution in section A-A. The red lines indicate the stress distribution across the cross section, the stress profile is not continuous due to the stiffness mismatch.

$$F_1 = E_m \frac{\Delta L_1}{a_1} t_m b \tag{5}$$

where a_1 is the interfacial crack length andΔL_1 is the extension of the metallic ligament which can be found from the tensile deformation in the ligament:

$$\Delta L_1 = \int_0^{a_1} d_{1,1} d\theta = \int_0^{a_1} \frac{d_{1,1}\left(0.5P(L-x) - F_1 d_{1,1}\right)}{(EI)_1} dx \tag{6}$$

where $d_{1,1}$ is the distance of the debonded metallic layer from the neutral axis. The crack growth can be taken into account through the compliance method assuming linear elastic fracture mechanics (LEFM). Under displacement-control conditions, the compliance method gives an equation for the energy release rate when no plastic deformation occurs in metallic layers:

$$G = \frac{P^2}{8b} \frac{\partial C}{\partial a_1} \tag{7}$$

where the factor 1/8 accounts for the propagation of 4 interfacial cracks after the fracture of the ceramic layer, and where C is the compliance of the beam which can be evaluated as the maximum displacement of the beam $\delta_2|_{x=L}$ divided by the applied load:

$$C = \frac{\delta_2|_{x=L}}{P} \tag{8}$$

Assuming that the center of the beam subjected to three-point bending loads is stationary while the supports move upwards $\delta_1 = 0$ and $\delta_1^{'} = 0$, we find the values of the constants $A_1 = 0$ and $B_1 = 0$. Likewise, for the damaged zone, we impose the boundary conditions $\delta_1|_{x=a_1} = \delta_2|_{x=a_1}$ and $\delta_1^{'}|_{x=a_1} = \delta_2^{'}|_{x=a_1}$ at the boundary with the intact zone ($x = a_1$). This results in:

$$A_2 = \frac{(EI)_2}{(EI)_1}\left(\frac{P}{2}\left(La_1 - \frac{{a_1}^2}{2}\right) - F_1 d_{1,1} a_1\right) - \frac{P}{2}\left(La_1 - \frac{{a_1}^2}{2}\right) \tag{9}$$

$$B_2 = \frac{(EI)_2}{(EI)_1}\left(\frac{P}{2}\left(L\frac{{a_1}^2}{2} - \frac{{a_1}^3}{6}\right) - F_1 d_{1,1}\frac{{a_1}^2}{2}\right) - \frac{P}{2}\left(L\frac{{a_1}^2}{2} - \frac{{a_1}^3}{6}\right) - A_2 a_1 \tag{10}$$

Interfacial crack propagation ends when the crack driving force G reaches its critical value G_c. We write the nondimensional form of the critical energy release rate as:

$$G^* = \frac{12 G_c (EI)_{eq}}{b t^4 S_c^2} \tag{11}$$

We can now form a system of equations that governs the mechanical response of a multilayered beam with a broken layer. The location of the neutral axis in damaged zone, c_1, and the applied force P are the unknowns, which we can obtain from the equations of equilibrium and of displacement of the beam. We solve the system of equations, numerically. First, the input of our model are the displacement at which the first ceramic layer breaks $\delta_2|_{x=L}$ as well as an initial guess for the interfacial crack length a_1. Then the system of equations is solved and the energy release rate evaluated. We adjust the crack length according to the energy criterion for crack propagation and repeat the procedure. The next intact layer fractures once its stress exceeds its strength, else we increase the displacement and repeat the procedure until the next ceramic layer breaks. The system of equation includes the equilibrium of the forces and the equation of the displacement of the beam.

$$\begin{bmatrix} \int \sigma(y) dA + F1 \\ \delta - \delta_2|_{x=L} \end{bmatrix} = 0 \tag{12}$$

3.2. Failure of several ceramic layers

To maximize the properties of the multilayered beam, we need to obtain the entire load-displacement curve of the beam in bending, which involves the failure of multiple ceramic layers. The equations presented above for the case of a single failed ceramic layer can be generalized to study the beam with N_{broken} broken ceramic layers. The load-displacement equation can be rewritten as:

$$(EI)_n \delta_n(x) = \frac{P}{2}\left(L\frac{x^2}{2} - \frac{x^3}{6}\right) - \sum F_i d_{i,n} \frac{x^2}{2} + A_n x + B_n \tag{13}$$

The general boundary conditions are those of the beam with one broken ceramic layer resulting in $A_1 = B_1 = 0$. To find the constants for the other zones, namely A_n and B_n, we impose the boundary conditions of the beam with one broken layer, i.e. between two adjacent zones we have: $\delta_n|_{x=a_{n-1}} = \delta_{n-1}|_{x=a_{n-1}}$ and $\delta_n'|_{x=a_{n-1}} = \delta_{n-1}'|_{x=a_{n-1}}$.

To find the location of the neutral axis in each region, we need to write the equation for the equilibrium of forces for all regions except the last region where the location of neutral axis is known. With N_{broken} cracked ceramic layer:

$$\int \sigma(y) dA + \sum F_i = 0 \tag{14}$$

where σ, and A are respectively the stress distribution, and the area of the cross section in each region. The extension of each debonded metallic ligament can be obtained from:

$$\Delta L_i = \int_0^{a_i} \frac{d_{i,n}\left(0.5{*}P{*}(L-x) - \sum F_i d_{i,n}\right)}{(EI)_n} dx \tag{15}$$

Finally, we use the equation above, i,e, the extension in each layer, to find the force in each ligaments as:

$$F_i = E_m \frac{\Delta L_i}{a_i} t_m b \tag{16}$$

The energy release rate can be written as:

$$G = \frac{P^2}{8b} \frac{\partial C}{\partial a_i} \tag{17}$$

where i is the crack number. The compliance of the beam is obtained from:

$$C = \frac{\delta_{Nbroken+1}|_{x=L}}{P} \tag{18}$$

where $\delta_{Nbroken+1}|_{x=L}$ is the displacement at the supports. We can then form the following system of equations:

Damaged zone 1

$$\text{Damaged zone } n \begin{bmatrix} \int \sigma(y)dA + F1 \\ \vdots \\ \int \sigma(y)dA + F_1 + F_2 + \ldots + F_{Nbroken-n+1} \\ \vdots \\ \int \sigma(y)dA + 0 \\ \delta - \delta_{Nbroken+1}|_{x=L} \end{bmatrix} \quad (19)$$

Intact zone

For simplicity we assume that crack propagation only occurs at the two interfaces between one broken ceramic layer and its adjacent metallic layers, whereas other existing cracks do not extend. We start the analysis by applying an energy-based criterion for propagation from the tips of the newly formed cracks. We assess the condition for crack propagation starting from the newly-formed crack. We repeat this procedure for all cracks until the energy available for crack growth is exhausted (Fig. 4). Then, we evaluate the stress in the next intact layer, and increase the displacement accordingly. We repeat this procedure until the last ceramic layer fractures, i.e. the complete failure of the beam (Fig. 4).

3.3. Typical load-deflection curve

Fig. 5 shows two typical load-deflection curves predicted by our models, along with snapshots of the model. The initial response is linear elastic, up to a first peak load when the first ceramic layer breaks. This is followed by a sharp load drop in force. As the displacement increases both the force and the debonding lengths increase until the stress in the next intact ceramic layer exceeds the strength of the ceramic. When new ceramic layers break new interfacial cracks are formed and the curve experiences multiple sequences of sharp drops and slow increase in force. Eventually all layers break, a process that leads to the complete failure of the beam. Illustrated in Fig. 5 is also the difference in the beam response to different values of interfacial toughness. Low interfacial

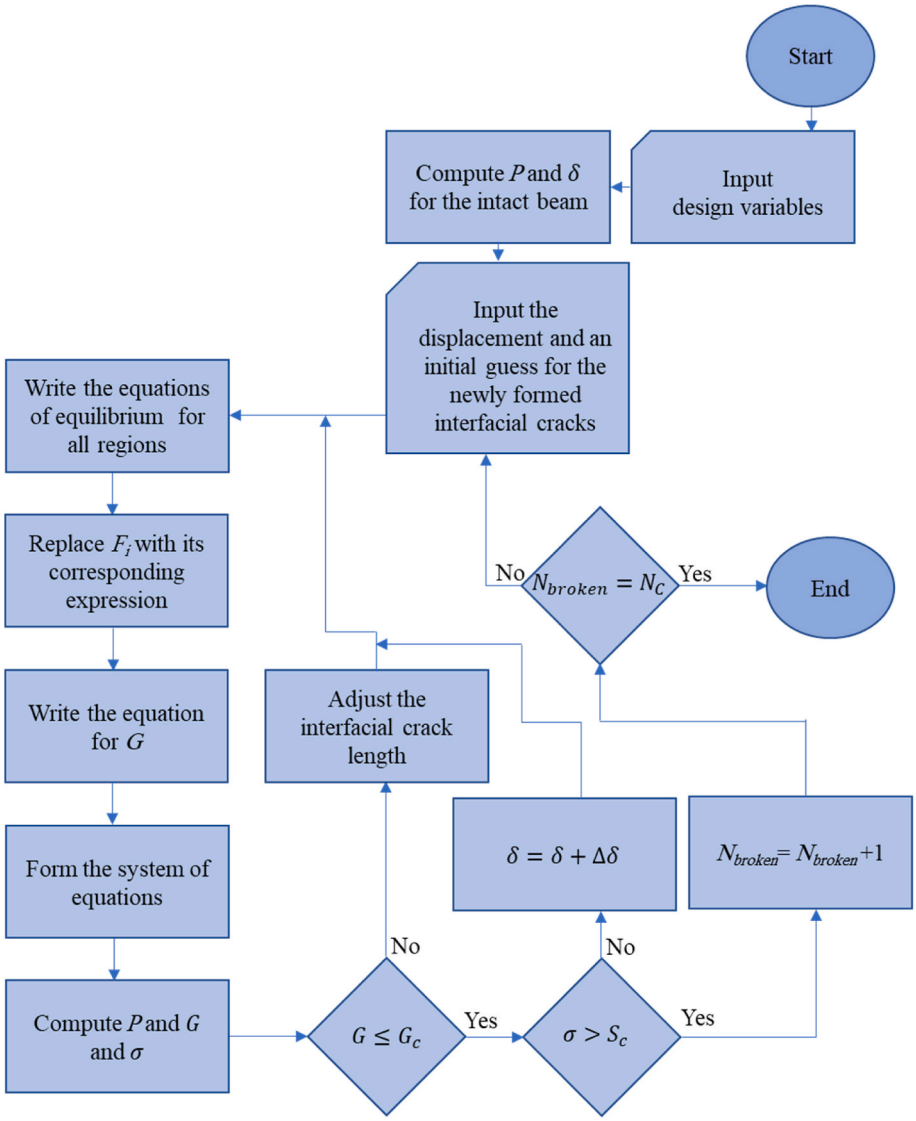

Fig. 4. Flowchart showing the procedure to follow for the implementation of the numerical model proposed in this work.

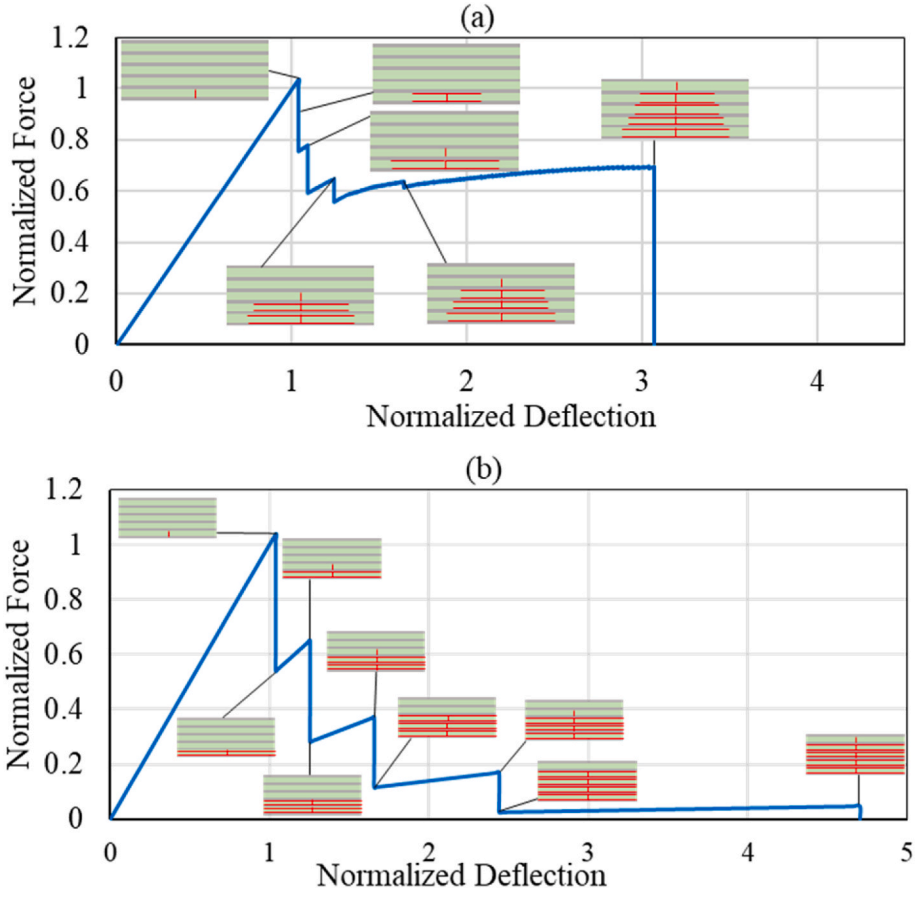

Fig. 5. Force-deflection curve for a multilayered beam with (a) intermediate interfacial toughness $G^* = 0.02$ (no full delamination) (b) low interfacial toughness $G^* = 0.001$ (all layers are delaminated).

toughness leads to sharper load drops while the beam with tougher interfaces can keep the load at higher magnitudes. Furthermore, low interfacial toughness allows for longer cracks along the interface so that the beam with low interfacial toughness exhibits higher deflection before complete failure.

4. Results

The ultimate goal of this work is to improve the architecture of a layered metal/ceramic composite which offers enhanced mechanical properties, high strength, stiffness and toughness. Here we discuss the effects of changes in variables including effective stiffness ratio, interfacial toughness, volume fraction of the reinforcement, and the number of layers on the mechanical response of the multilayered structure.

4.1. Strength

We take the peak load of each force-deflection diagram as the strength of the beam. Fig. 6 shows the flexural strength of the beam as function of the ratio of elastic modulus for given number of layers and volume fractions. Overall, stiffer reinforcements, achieved with high E_m/E_c, lead to higher strength because stiffer metallic layer carry more of the flexural stresses, effectively shielding the ceramic layers from failure. Here, the beams with smaller number of layers and higher volume fraction of metallic phase, both of which most effectively increase the bending stiffness of the beam, carry larger loads before the failure of the first ceramic layer. However, reinforcing the beams with a metal with lower relative stiffness adversely affects the bending stiffness of the beam. In this case, higher number of layers and lower volume fractions have less negative effect on the bending stiffness of the beam, so that the

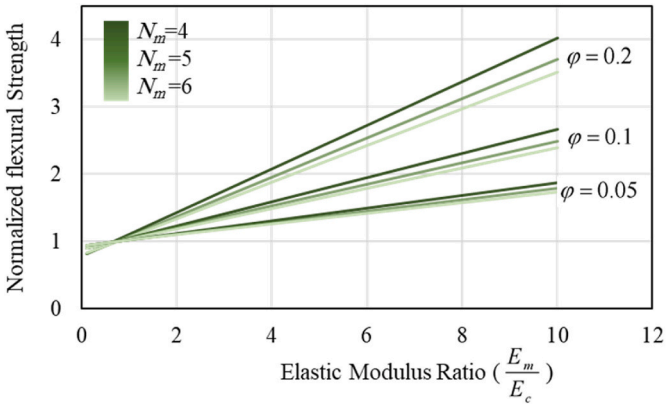

Fig. 6. Variation of Strength and stiffness with respect to the input variables.

beam exhibits higher stiffness and strength.

The maximum load is the first peak load for all the combinations of the design variables with some exceptions. For example, the beams with $E_m/E_c = 10$ and high interfacial toughness exhibit a second peak slightly higher than the first peak (Fig. 7a). In other words, a partially failed beam is able to carry higher loads than an intact beam. While short interfacial cracks length keeps the compliance of the beam, the debonded metallic ligaments bridging the through-thickness crack exert large forces on the main crack faces. These high forces resulting from the high stiffness of the metal shield the next intact ceramic layer from failure (by reducing the stress), so that the beam carries higher loads. These results indicate that to attain a higher second peak in a multilayered beam, a

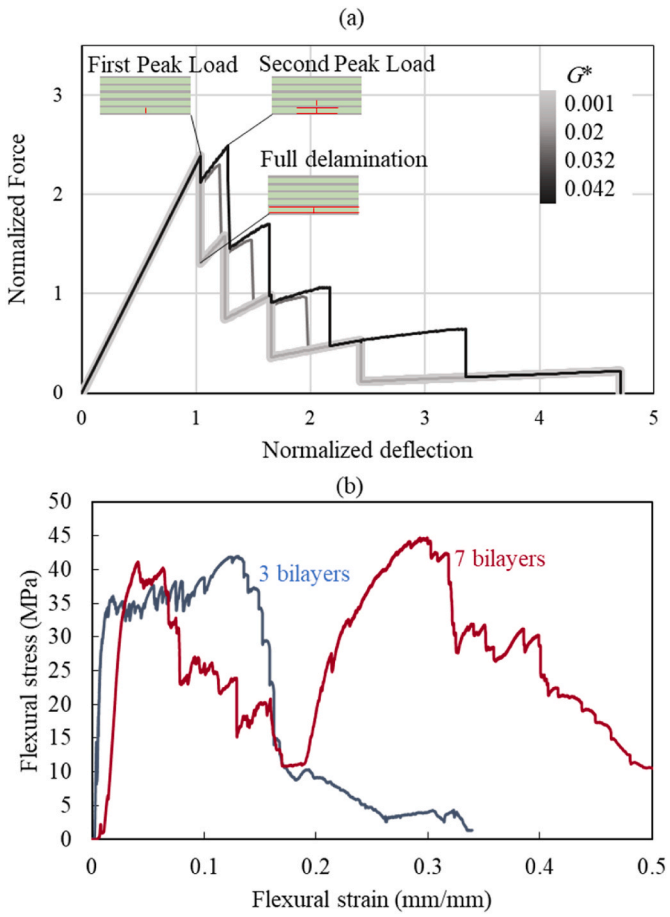

Fig. 7. Load-displacement curves (a) for the beams with $N_m = 6$, $\varphi = 0.1$, $E_m/E_c = 10$, and different interfacial toughness obtained from the model (b) for the beams with three and seven bilayers of titanium mesh obtained from experiment (Cavelier et al., 2021).

high-stiffness reinforcement is required.

Another requisite to achieve a second peak load larger in magnitude than the first one is that the toughness of the interface should be high enough to arrest long crack advances and low enough to allow for crack deflection. This phenomenon was also observed in the experiments conducted in our previous work (Cavelier et al., 2021) where titanium mesh/CS multilayers showed peaks with higher amplitudes than the first peak load (Fig. 7b). With other combinations of design parameters, however, the model predicts that the subsequent peaks are smaller in magnitude.

4.2. Dissipated energy

Damage tolerant materials are able to dissipate a substantial amount of energy before failure. Here our goal is to tailor the design parameters to maximize the energy dissipation of the multilayered beam. The amount of the energy dissipated is simply computed as the area under the load-deflection curve. Fig. 8 shows the predicted variations of dissipated energy with respect to the toughness of the interface for given volume fractions of the metallic phase. We also subclassify the results based on the elastic modulus ratio and the number of the layers. We do not show the results for $\varphi = 0.2$ since they follow the same trend as the results for $\varphi = 0.1$. While the effect of number of layers on the response of the multilayered material is independent of other parameters, the effect of interfacial toughness on the behavior of the multilayers should be studied in conjunction with other variables including the stiffness ratio and the volume fraction of the metallic phase. Therefore, we first discuss the effect of number of layers and then we explain how other parameters influence the failure behavior of the beam.

4.2.1. Effect of number of layers

The model predicts that the beam with higher number of layers dissipates larger amount of energy since the number of interfaces that contribute to the energy dissipation and the number of debonded metallic ligaments are higher. Fig. 9a shows that the lower the number of layers, the larger the magnitude of load drops, thus implying that the beam loses higher portion of its load bearing capacity. The effect of number of layers on energy dissipation, however, is less notable in the case of the beams reinforced with a metal with lower relative stiffness, especially at high interfacial toughness when the structure response approaches the behavior of a monolithic brittle material. In this case, too tough interfaces lead to a large initial load drop, resulting from the failure of multiple ceramic layers at the same deflection (Fig. 9b). This is because neither the fracture of the previous brittle layers nor the interfacial crack propagation are sufficient to reduce the stress in the adjacent intact ceramic layers. Therefore, not only does the load drop shrink the area under the load-deflection curve, but also the beam has less intact layers to carry more loads.

4.2.2. Effect of interfacial toughness and volume fraction of the metal

The above brings us to the next part of the discussion where we explain the effects of the interfacial toughness and the volume fraction of the metal on the response of the system with respect to the stiffness ratio. In the case that the metallic phase has lower relative stiffness ($E_m/E_c = 0.1$), the results demonstrate that forming ceramics into multilayered structures can increase the energy dissipation regardless of the volume fraction of the metallic phase, provided that the interfacial toughness is not too high. At low interfacial toughness, the crack deflects into the interfaces once each ceramic layer breaks, preventing catastrophic failure. Interfacial crack propagation reduces the stress in the next intact ceramic layer while increasing the compliance of the beam resulting in load drops as well (Fig. 9b). This increase in the energy dissipation is followed by a decrease if the interfaces are too tough. In the case of strongly bounded layers, the structure exhibits a brittle-like behavior. As mentioned in the above, this brittle-like failure behavior is due to the stress in the next intact brittle layers reaching the ceramic strength despite the interfacial crack propagation and fracture of the previous ceramic layers, so that all brittle layers fail at the same deflection. In addition, these beams tolerate smaller loads in comparison to the reference material. Therefore, packing the ceramic layers and metallic layers with lower relative stiffness with tough interfaces has a detrimental effect on both the strength and energy dissipation of the structure. This behavior has also been observed for layered ceramic as well: multilayer structures made of brittle materials with the layers strongly packed together also show the behavior of a monolithic material as the crack can propagate to the next layer readily (Folsom et al., 1994a).

The response of the beams with $E_m/E_c = 1$ depends on both the volume fraction of the metal and the interfacial toughness. At low volume fraction, the results show (Fig. 8a) a peak point (ascending-descending trend), whereas at high volume fraction, the energy dissipation follows an ascending trend with respect to the toughness of the interface (Fig. 8b). The reason for this behavior is that at high volume fraction of metallic phase, the increase in the interfacial toughness leads to the crack arrest delaying or preventing the full delamination. Therefore, the beam has higher load-bearing capacity and can keep the load at higher magnitudes, so that the energy dissipation keeps rising with the increase in the toughness of the interfaces (Fig. 9c). However, the simultaneous fracture of high number of ceramic layers in the beams with low values of volume fraction of metal and with strongly bounded layers shrinks the area under the load displacement curve (Fig. 9d). As a result, the enhancement in the energy dissipation is followed by a decline.

The last case pertains to beams reinforced with metals with high

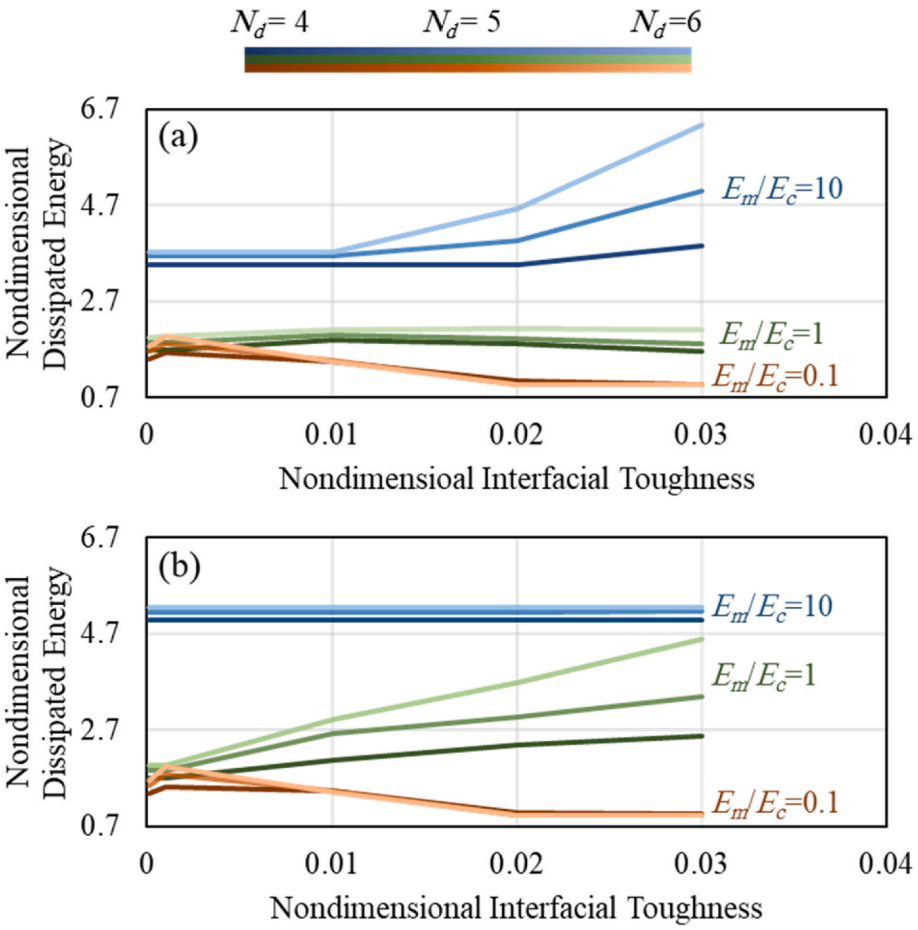

Fig. 8. Effect of input variables, N_m, G^*, and E_m/E_c, on the amount of nondimensional dissipated energy for (a) $\varphi = 0.05$ (b).$\varphi = 0.1$

effective stiffness ($E_m/E_c = 10$). At low volume fraction ($\varphi = 0.05$), the amount of dissipated energy raises with the increase in the interface toughness. This is because the cracks travel shorter distances in tougher interfaces, maintaining the beam compliance, so that the entire beam can keep the load at higher magnitudes. However, at higher volume fractions ($\varphi > 0.05$), the toughness of the interface has no effect on the energy dissipation due to the relatively high amount of energy released as the interfacial cracks propagate, a process that drives the cracks to the ends of the beam. In other words, the interfaces are not tough enough to arrest the propagating cracks leading to the full delamination of each metallic layer immediately after the fracture of each ceramic layer. As a result, the response of the beams with dissimilar interfacial toughness to the flexural loads does not change, as shown in Fig. 7a, where the load-displacement curves of the beams with $G^* = 0.001$ and $G^* = 0.02$ coincide.

Fig. 8 also indicates that while the increase of the stiffness ratio improves the energy dissipation in most of the cases, there is an exception where the beam with $E_m/E_c = 0.1$ dissipates approximately as much energy as the beam with $E_m/E_c = 1$ at $G^* = 0.001$. At this nondimensional value of the interfacial toughness, the energy dissipation for the beam with $E_m/E_c = 0.1$ is at its highest value. This occurs because the high crack driving force delaminates entirely the metallic ligaments in the beam with $E_m/E_c = 1$, thus increasing the compliance of the beam and leading to large load drops once each ceramic layer breaks. On the other hand, the interfacial crack arrest takes place, enabling the beam $E_m/E_c = 0.1$ to dissipate a relative high amount of energy.

5. Summary

In this paper, we studied the post fracture bending behavior of a series of multilayered beam by manipulating several design parameters, including the toughness of the interface, the thickness ratio, the materials stiffness, and the number of layers, to the model. The ultimate goal was to promote crack deflection and crack bridging in order to improve the energy dissipation and strength of a CS bone graft material. We proposed a numerical model which predicts that a layered bone graft material with higher number of layers can dissipate higher amounts of energy while its strength depends on the effective stiffness ratio: a lower number of layers is desired for high effective stiffness ratio. While increasing the effective stiffness ratio leads to an increase in both energy dissipation and strength, it also results in the full delamination after the fracture of each ceramic layer, a phenomenon which can be controlled at low volume fractions of reinforcement. Our model also predicts that a beam with tuned architecture can exhibit a second peak load higher than the first one.

All the results can be presented as a chart that provides guidelines for designing a damage tolerant multilayered bone graft material which could offer high values of strength, stiffness and dissipated energy. The chart shows how different variables such as effective stiffness, interfacial toughness, number of layers, and the volume fraction of the reinforcement affect the strength and damage tolerance of the multilayered structure, so that these parameters can be tuned to attain the required mechanical properties. To streamline the comparison between the results, we divide the results into three categories: $E_m/E_c = 0.1$, 1, 10. Fig. 10a, b, and c show each category and Fig. 10d is the combined chart

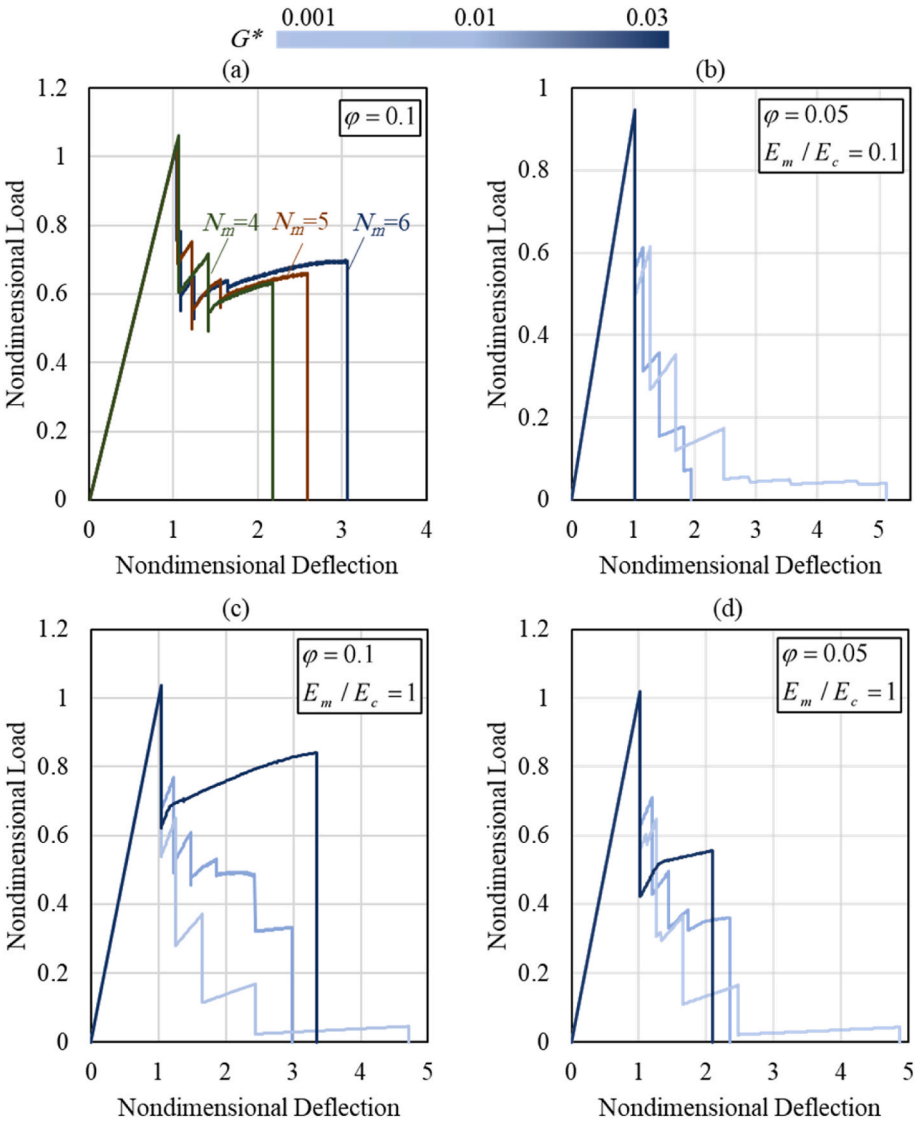

Fig. 9. Nondimensional load-deflection curves for the beams with six metallic layers. (a) The effect of number of layers. The effect of interfacial ratio on the beams with (b) $E_m/E_c = 0.1$ (c) $\varphi = 0.1$ (d).$\varphi = 0.05$

illustrating all the results together. Fig. 10a (respectively Fig. 10b and c) shows how lower (respectively higher) volume fraction and higher (respectively lower) number of layers of reinforcement leads to a higher strength when the metallic layers have lower (respectively higher) relative stiffness. As we previously explained, these parameters control the effective stiffness of the beam, and thereby control the strength. Fig. 10 also illustrates that while the effect of volume fraction on the energy dissipation depends on the relative stiffness ratio, a higher number of layers is always desired. The results also indicate that for a given effective stiffness ratio, the interfacial toughness can be tuned so that a beam with lower volume fraction of reinforcement dissipates higher amounts of energy than a beam reinforced with higher volume fractions of the metal. However, this is not always the case as when there is a large difference between the volume fraction of the reinforcement of the two beams, the beam with higher volume fraction is always stronger and more damage tolerant than its counterpart.

The lower left corner of the combined chart (Fig. 10d) is occupied by data points corresponding to the beams with $E_m/E_c = 0.1$. This area can be divided into two groups: one belongs to the beams with tough interfaces which exhibit deteriorated mechanical performance: low strength (due to low stiffness of metal) and low fracture resistance (due to the brittle-like behavior). The other one belongs to the beams with intermediate and low interfacial toughness which are more fracture tolerant than the pure ceramic while they are still less strong. The top-right part of the combined chart is occupied by the beams reinforced with $E_m/E_c = 10$. The N_m constant guidelines show that the multilayered material dissipates higher amounts of energy at the cost of losing strength by the increase in the number of layers. For a given number of layers, raising the volume fraction of the reinforcement leads to higher strength and energy dissipation. For values of the effective elastic modulus $E_m/E_c = 1$ and 0.1, the slope of N_m constant lines indicating the rate at which the strength changes with the change energy dissipation is negligible.

Outstanding biodegradability and osteoconductivity of CS make it a potent candidate for bone grafting applications. In our previous work (Cavelier et al., 2021), we have numerically and experimentally demonstrated that reducing the porosity of CS as well as incorporating ductile interlayers into CS can significantly enhance its mechanical performance. In this paper, we have developed a more refined model to predict the fracture behavior of the ceramic/metal structure. The model considers the effects of more variables such as the interfacial toughness into account. Our model indicates that the effect of variables cannot be studied independently because a change in a variable changes the effect of other parameters on the mechanical response of the multilayer to the

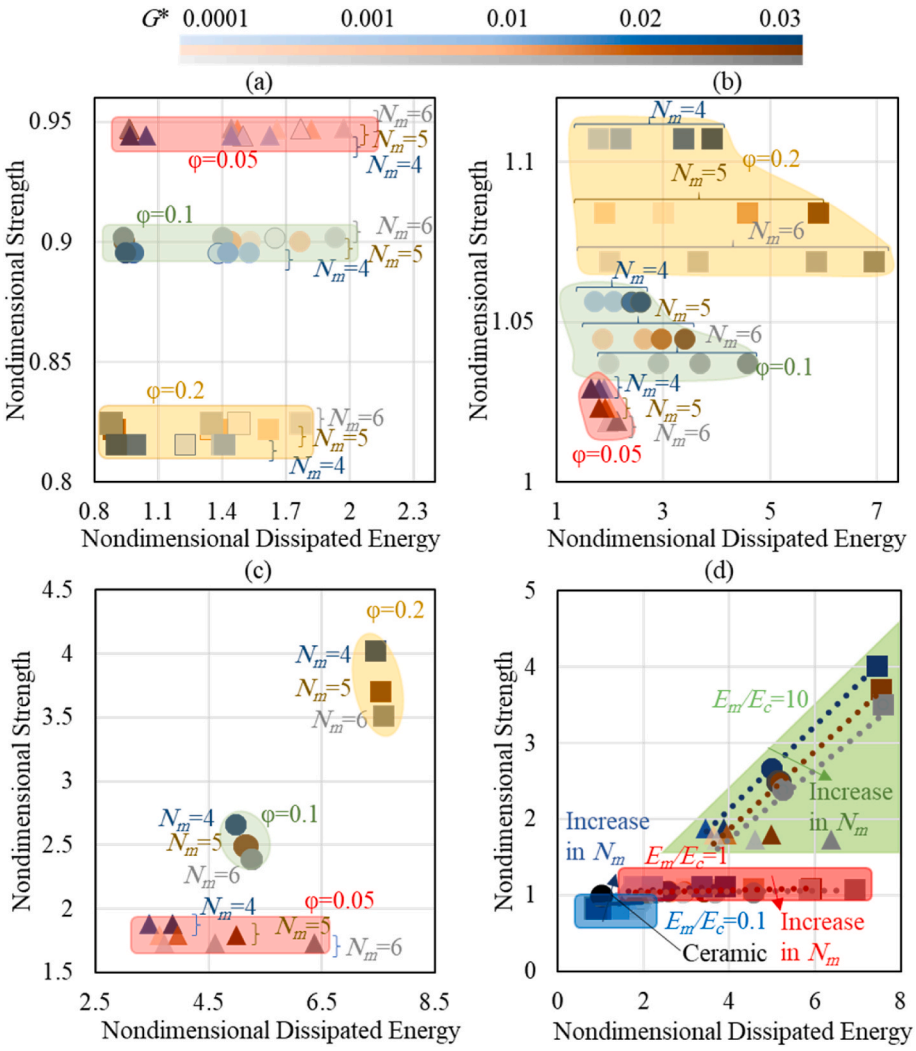

Fig. 10. Strength-dissipated energy chart comparing the effect of the parameters, number of layers, effective stiffness, interfacial toughness, and volume fraction of the reinforcement on the properties of a multilayered beam with (a) $E_m/E_c = 0.1$ (b) $E_m/E_c = 1$ (c) $E_m/E_c = 10$ (d) combined chart.

flexural loads. For example, the effect of interfacial toughness on the energy dissipation varies with the value of the effective stiffness ratio. Moreover, the model we have presented here gives tighter control on the designing of the architecture and the tuning of the behavior of multilayered bone graft materials. Our model predicts that higher number of layers to enhance damage tolerance, and a reinforcement with high stiffness to enhance both strength and energy dissipation are desired (Fig. 10d), a result aligned with previous work (Cavelier et al., 2021). At high effective stiffness ratio, however, the high strain energy release rate drives the interfacial cracks to the ends of the beam leading to load drops. Therefore, an optimal interfacial toughness causing crack arrest could enable the beam to keep the load at higher levels.

The effect of number of layers on the flexural stiffness is also in accordance with our previous experimental results where increasing the number of layers decreased the stiffness of the beam. Assuming that titanium meshes are stiffer than CS, we attribute the difference to the large number of imperfections present in the beams with high number of layers. These imperfections acted as stress concentrators where new cracks could appear leading to the decline in the stiffness of the samples. However, our model does not take the imperfections into account and predict that the increase in the number of layers makes the beams with high effective stiffness ratio compliant. The key points we can draw from our model are thus as follows:

- The response of multilayered system with $E_m/E_c = 0.1$ to flexural loads approaches that of a monolithic material if the layers are strongly bounded.
- The number of layers does not have significant effect on the fracture resistance of the beams with $E_m/E_c = 0.1$ at high interfacial toughness, and the beams with$E_m/E_c = 10$ at high volume fractions. In all other cases, the higher the number of layers, the higher the amount of dissipated energy. The role of the layer number on the strength and stiffness, however, depends on the effective stiffness ratio; lower (higher) number of layers are desired if the reinforcement is stiffer (less stiff) than the ceramic.
- The energy dissipation as a function of interfacial toughness for beams with $E_m/E_c = 0.1$ regardless of volume fractions, and with $E_m/E_c = 1$ at low volume fractions, exhibit an optimal value. The interfacial toughness has no effect on the energy dissipation when $E_m/E_c = 10$ at high volume fractions. The increase in the toughness of the interface leads to enhanced energy dissipation for beams with $E_m/E_c = 10$ and $E_m/E_c = 1$ at low and high volume fractions respectively.
- Our model predicts that the multilayered beam with the $\varphi = 0.2$, $E_m/E_c = 10$ exhibits the best mechanical performance: the beams with higher (lower) number of layers are preferred when energy dissipation (respectively strength) is a requirement.

Finally, in this paper we have demonstrated how the architecture of a metal/ceramic structure can be tailored to control and tune the fracture behavior of a multilayered bone graft material, so that it offers a combination of conflicting mechanical properties such as strength, stiffness, and damage tolerance essential for medical applications.

CRediT authorship contribution statement

Seyed Alireza Mirmohammadi: Investigation, Methodology, Writing – original draft. **Damiano Pasini:** Supervision, Writing – original draft. **Francois Barthelat:** Funding acquisition, Supervision, Writing – original draft, Resources.

Declaration of competing interest

The authors declare that they have no known competing financial interests or personal relationships that could have appeared to influence the work reported in this paper.

Acknowledgments

This project was supported by a Collaborative Health Research Projects grant from CIHR and NSERC. SAM was partially supported by a McGill Engineering Doctoral Award from the Faculty of Engineering at McGill University.

References

Anusavice, K.J., Shen, C., Rawls, H.R., 2012. Phillips' Science of Dental Materials. Elsevier Health Sciences.

Barthelat, F., 2015. Architectured materials in engineering and biology: fabrication, structure, mechanics and performance. Int. Mater. Rev. 60 (8), 413–430. https://doi.org/10.1179/1743280415Y.0000000008, 2015/11/17.

Barthelat, F., Yin, Z., Buehler, M.J., 2016. Structure and mechanics of interfaces in biological materials. Nat. Rev. Mater. 1 (4), 16007 https://doi.org/10.1038/natrevmats.2016.7, 2016/03/08.

Cavelier, S., Mirmohammadi, S.A., Barthelat, F., 2021. Titanium mesh-reinforced calcium sulfate for structural bone grafts. J. Mech. Behav. Biomed. Mater. 118, 104461 https://doi.org/10.1016/j.jmbbm.2021.104461, 2021/06/01/.

Chen, Z., Mecholsky Jr., J.J., 1993. Toughening by metallic lamina in nickel/alumina composites. J. Am. Ceram. Soc. 76 (5), 1258–1264. https://doi.org/10.1111/j.1151-2916.1993.tb03750.x, 1993/05/01.

Clegg, W.J., Kendall, K., Alford, N.M., Button, T.W., Birchall, J.D., 1990. A simple way to make tough ceramics. Nature 347 (6292), 455–457. https://doi.org/10.1038/347455a0, 1990/10/01.

Dey, A., Dey, P., Datta, S., Mukhopadhyay, A.K., Maiti, H.S., 2008. A new theoretical model for development of damage tolerant composites. Trans. Indian Ceram. Soc. 67 (2), 63–74. https://doi.org/10.1080/0371750X.2008.11078643, 2008/04/01.

Folsom, C.A., Zok, F.W., Lange, F.F., 1994a. Flexural properties of brittle multilayer materials: I, modeling. J. Am. Ceram. Soc. 77 (3), 689–696. https://doi.org/10.1111/j.1151-2916.1994.tb05350.x, 1994/03/01.

Folsom, C.A., Zok, F.W., Lange, F.F., 1994b. Flexural properties of brittle multilayer materials: II, experiments. J. Am. Ceram. Soc. 77 (8), 2081–2087. https://doi.org/10.1111/j.1151-2916.1994.tb07100.x, 1994/08/01.

Humburg, H., Volkmann, E., Koch, D., Müssig, J., 2014. Combination of biological mechanisms for a concept study of a fracture-tolerant bio-inspired ceramic composite material. J. Mater. Sci. 49 (23), 8040–8050. https://doi.org/10.1007/s10853-014-8511-x, 2014/12/01.

Hwu, K.L., Derby, B., 1999. Fracture of metal/ceramic laminates—II. Crack growth resistance and toughness. Acta Mater. 47 (2), 545–563. https://doi.org/10.1016/S1359-6454(98)00358-9, 1999/01/15/.

Khayer Dastjerdi, A., Rabiei, R., Barthelat, F., 2013. The weak interfaces within tough natural composites: experiments on three types of nacre. J. Mech. Behav. Biomed. Mater. 19, 50–60. https://doi.org/10.1016/j.jmbbm.2012.09.004, 2013/03/01/.

Koester, K.J., Ager, J.W., Ritchie, R.O., 2008. The true toughness of human cortical bone measured with realistically short cracks. Nat. Mater. 7 (8), 672–677. https://doi.org/10.1038/nmat2221, 2008/08/01.

Kovar, D., Thouless, M.D., Halloran, J.W., 1998. Crack deflection and propagation in layered silicon nitride/boron nitride ceramics. J. Am. Ceram. Soc. 81 (4), 1004–1112. https://doi.org/10.1111/j.1151-2916.1998.tb02438.x, 1998/04/01.

Krstic, V.D., 1983. On the fracture of brittle-matrix/ductile-particle composites. Philos. Mag. A 48 (5), 695–708. https://doi.org/10.1080/01418618308236538, 1983/05/01.

Lenčéš, Z., Hirao, K., Brito, M.E., Toriyama, M., Kanzaki, S., 2000. Layered silicon nitride-based composites with discontinuous boron nitride interlayers. J. Am. Ceram. Soc. 83 (10), 2503–2508. https://doi.org/10.1111/j.1151-2916.2000.tb01582.x.

Li, M., Soboyejo, W.O., 2000. An investigation of the effects of ductile-layer thickness on the fracture behavior of nickel aluminide microlaminates. Metall. Mater. Trans. 31 (5), 1385–1399. https://doi.org/10.1007/s11661-000-0257-1, 2000/05/01.

Ming-Yuan, H., Hutchinson, J.W., 1989. Crack deflection at an interface between dissimilar elastic materials. Int. J. Solid Struct. 25 (9), 1053–1067. https://doi.org/10.1016/0020-7683(89)90021-8, 1989/01/01/.

Moussa, H., et al., 2020. Selective crystal growth regulation by chiral α-hydroxycarboxylic acids improves the strength and toughness of calcium sulfate cements. ACS Appl. Bio Mater. 3 (12), 8559–8566. https://doi.org/10.1021/acsabm.0c00918, 2020/12/21.

Phillipps, A.J., Clegg, W.J., Clyne, T.W., 1993. Fracture behaviour of ceramic laminates in bending—I. Modelling of crack propagation. Acta Metall. Mater. 41 (3), 805–817. https://doi.org/10.1016/0956-7151(93)90014-J, 1993/03/01/.

Ritchie, R.O., 2011. The conflicts between strength and toughness. Nat. Mater. 10 (11), 817–822. https://doi.org/10.1038/nmat3115, 2011/11/01.

Thurner, P.J., et al., 2010. Osteopontin deficiency increases bone fragility but preserves bone mass. Bone 46 (6), 1564–1573. https://doi.org/10.1016/j.bone.2010.02.014, 2010/06/01/.

Tomaszewski, H., Węglarz, H., Wajler, A., Boniecki, M., Kalinski, D., 2007. Multilayer ceramic composites with high failure resistance. J. Eur. Ceram. Soc. 27 (2), 1373–1377. https://doi.org/10.1016/j.jeurceramsoc.2006.04.030, 2007/01/01/.

Wang, C.-a., Huang, Y., Zan, Q., Zou, L., Cai, S., 2002. Control of composition and structure in laminated silicon nitride/boron nitride composites. J. Am. Ceram. Soc. 85 (10), 2457–2461. https://doi.org/10.1111/j.1151-2916.2002.tb00480.x, 2002/10/01.

Ye, F., Liu, S., Hu, S., Yang, H., Liu, Q., Zhang, B., 2015. A route to increase fracture toughness of layered Si3N4/SiC composite using interlocked interfaces. Ceram. Int. 41 (8), 10331–10335. https://doi.org/10.1016/j.ceramint.2015.04.102, 2015/09/01/.

Zan, Q., Wang, C.-a., Huang, Y., Zhao, S., Li, C., 2004. Effect of geometrical factors on the mechanical properties of Si3N4/BN multilayer ceramics. Ceram. Int. 30 (3), 441–446. https://doi.org/10.1016/S0272-8842(03)00129-9, 2004/01/01/.

Zhang, W., Telle, R., Uebel, J., 2014. R-curve behaviour in weak interface-toughened SiC-C laminates by discrete element modelling. J. Eur. Ceram. Soc. 34 (2), 217–227. https://doi.org/10.1016/j.jeurceramsoc.2013.08.021, 2014/02/01/.

Zok, F., Hom, C.L., 1990. Large scale bridging in brittle matrix composites. Acta Metall. Mater. 38 (10), 1895–1904. https://doi.org/10.1016/0956-7151(90)90301-V, 1990/10/01/.